J. Sens. Sens. Syst., 7, 207–217, 2018
https://doi.org/10.5194/jsss-7-207-2018

JSSS Journal of Sensors and Sensor Systems Open Access

High-resolution ultrasonic spectroscopy

Vitaly Buckin

School of Chemistry, University College Dublin, Dublin, Belfield, Dublin 4, Ireland

Correspondence: Vitaly Buckin (vitaly.buckin@ucd.ie)

Received: 30 November 2017 – Accepted: 15 January 2018 – Published: 29 March 2018

Abstract. High-resolution ultrasonic spectroscopy (HR-US) is an analytical technique for direct and non-destructive monitoring of molecular and micro-structural transformations in liquids and semi-solid materials. It is based on precision measurements of ultrasonic velocity and attenuation in analysed samples. The application areas of HR-US in research, product development, and quality and process control include analysis of conformational transitions of polymers, ligand binding, molecular self-assembly and aggregation, crystallisation, gelation, characterisation of phase transitions and phase diagrams, and monitoring of chemical and biochemical reactions. The technique does not require optical markers or optical transparency. The HR-US measurements can be performed in small sample volumes (down to droplet size), over broad temperature range, at ambient and elevated pressures, and in various measuring regimes such as automatic temperature ramps, titrations and measurements in flow.

1 Introduction

Analytical capabilities available for real-time non-destructive monitoring of molecular processes in a variety of media, from solutions to emulsion, suspensions, and gels, are an important factor in modern developments in the pharmaceutical, food, chemical, biotechnological and other industries as well as in relevant academic research. A variety of "electromagnetic" spectroscopic techniques such as infrared, Raman, fluorescence, and UV–VIS are utilised for this purpose (see for example Svanberg, 2003). However, the efficiency of these spectroscopies is dependent on the optical transparency of the medium and is affected by light scattering in dispersions. In mixtures, these techniques often have a limited dynamic range (concentration of solutes). In addition, UV–VIS and fluorescence spectroscopies require optical activity of the molecules involved in analysed processes, and in their absence, the analysis is more complicated as chromogenic and fluorogenic markers are needed.

High-resolution ultrasonic spectroscopy is a relatively novel alternative to electromagnetic spectroscopy, applicable for precision, real-time, non-invasive monitoring of molecular and micro-structural transformations in solutions and complex dispersions. This ultrasonic spectroscopy employs high-frequency (MHz range) waves of compressions and decompressions (longitudinal deformations), which probe the elastic properties of materials determined by the intermolecular interactions and the micro-structural organization (Kudryashov et al., 2003). As ultrasonic waves propagate through most materials, this spectroscopy does not require optical transparency. Although ultrasonic spectroscopy has been utilised for material analysis for a long time and has demonstrated various successful applications (Povey and Mason, 1998; Povey, 1997; Holmes and Povey, 2017), the capability of this technique in analysis of molecular processes has been restricted by a number of factors. These include limited resolution and precision in measurements of ultrasonic parameters, the requirement for large sample volumes and often complicated measuring procedures. The development of high-resolution ultrasonic spectroscopy (HR-US), based on advances in the principles of ultrasonic measurements, electronics, and digital signal processing, surpasses these limitations (Buckin and O'Driscoll, 2002). This paper outlines the underlying principles of the HR-US technique and discusses examples of its application for real-time monitoring of molecular transformations in solutions and complex dispersions.

2 Measuring parameters

High-resolution ultrasonic spectroscopy utilises ultrasonic waves of longitudinal deformations of low amplitude traversing the analysed samples as illustrated in Fig. 1. Propagation of such waves over axis x in homogenous (within the length scale of the ultrasonic wave, "long-wavelength" regime) isotropic visco-elastic material can be presented as an oscillating displacement of the medium, $X(x,t)$, around its original (unstrained) position x (Lagrange description of motion; Morse and Ingard, 1986) with time t. For a wave of small amplitude (linear regime) $X(x,t)$ obeys the following wave equation:

$$\frac{\partial^2 X(x,t)}{\partial t^2} = \frac{M}{\rho_I}\frac{\partial^2 X(x,t)}{\partial x^2}, \quad (1)$$

where M is the complex modulus of longitudinal deformation composed of the volume or bulk, K_V, and the shear, G, moduli ($M = K_V + \frac{4}{3}G$), and ρ_I is the complex inertial density of the medium representing the ratio between the force applied to a small part of the medium and the acceleration caused by the force, calculated per unit of volume of the medium (Buckin, 2012; Buckin and Hallone, 2012). For periodic oscillations of X at $x = 0$ (boundary conditions) with frequency, f, the solution of Eq. (1) corresponding to a wave propagating in the direction of axis x can be presented in complex notations as follows:

$$X = X_0 e^{-\alpha x} e^{i2\pi f\left(t-\frac{x}{u}\right)}, \quad (2)$$

where X_0 is the amplitude of the wave at $x = 0$, α is the ultrasonic attenuation, u is the ultrasonic velocity, $\lambda = \frac{u}{f}$ is the wavelength of the ultrasonic wave and $i(=\sqrt{-1})$ is the imaginary constant. Combination of Eqs. (1) and (2) produces the relationship between the ultrasonic velocity and the attenuation and M and ρ_I:

$$\frac{u^2}{\left(1 - i\frac{\alpha\lambda}{2\pi}\right)^2} = \frac{M}{\rho_I}. \quad (3)$$

Separation of real and imaginary parts of this equation provides the system of two equations relating ultrasonic velocity and attenuation with the real and imaginary parts of M and ρ_I.

The ultrasonic attenuation represents the energy losses associated with the propagation of ultrasonic waves. In liquid dispersions, composed of particles in a solvent (continuous medium), several contributions to attenuation can be distinguished: classical (α_{class}), scattering (α_{scatt}) and intrinsic (α_{in}). In non-concentrated dispersions with a limited level of attenuation ($\frac{\alpha\lambda}{2\pi} \ll 1$), these contributions are expected to be additive: $\alpha = \alpha_{\text{class}} + \alpha_{\text{in}} + \alpha_{\text{scatt}}$ (see Buckin and Altas, 2017 for overview of the underlying relationships). The classical attenuation, α_{class}, represents the energy losses in the "shear part" of the longitudinal deformation of the medium

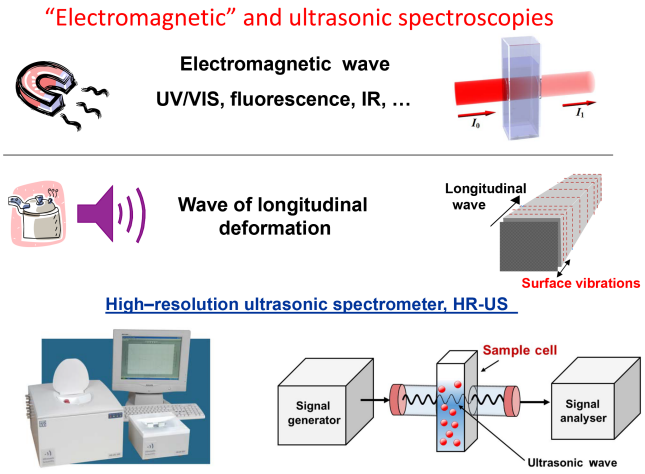

Figure 1. Illustration of principles of high-resolution ultrasonic spectroscopy.

in the wave (viscous losses) and the energy losses caused by the heat flow between the parts of ultrasonic wave of different temperature. The intrinsic attenuation, α_{in}, is composed of the contribution of the structural relaxation in the solvent and in the particles (Litovitz and Davis, 1964) and of the relaxation processes in fast chemical reactions. These contributions originate from the oscillations of the equilibrium in the molecular transformations (e.g. chemical reactions, conformational or structural rearrangements) caused by the oscillations of pressure and temperature in the ultrasonic wave; α_{scatt} characterises the energy losses caused by the scattering effects in the presence of particles (non-homogeneity in general) in the media. This includes the scattering of the ultrasonic wave and the two other waves, shear and thermal. The shear and thermal waves originate at the border between the particle and the continuous medium by the oscillating relative motion of the particles and the continuous medium, and by the oscillating temperature gradient at the border. The magnitude of the scattering attenuation is determined by the physical properties of the particle and the continuous medium and by the ratio of the size of the particle and the wavelength of the particular wave. Figure 2 illustrates the dependence of the wavelength of the three waves on the frequency in water and two organic solvents, ethanol and isooctane. As can be seen from the figure, at frequencies below 100 MHz, the wavelength of the ultrasonic wave is at the level of 10 µm and larger. Therefore, for nano-sized dispersions, the contribution of the scattering of this wave to attenuation can be neglected. Consequently, α_{scatt} at this long-wavelength regime is determined by the thermal and the shear (visco-inertial) effects. Figure 2 illustrates the dependence of the ultrasonic attenuation per wavelength at frequency 10 MHz, including its thermal and the visco-inertial components, on the radius of hydrated protein particles suspended in water at concentration of protein 1 % (w/w) and

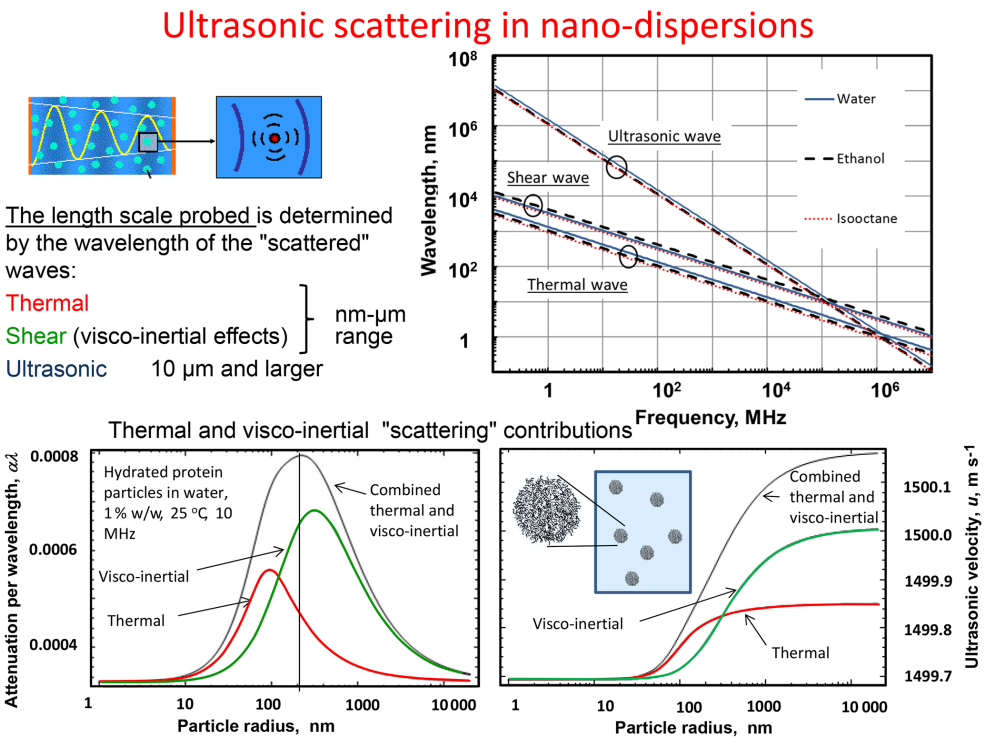

Figure 2. Ultrasonic scattering effects in nano-dispersions. Dependence of ultrasonic attenuation per wavelength, $\alpha\lambda$, and ultrasonic velocity, in suspensions of hydrated protein particles (at constant concentration) on their radius in water at 25 °C at 10 MHz frequency calculated with HR-US particle size module (Sonas technologies Ltd. Dublin); the physical properties of the protein particles and of water were provided with the software. The hydration level of protein (water-to-protein ratio) is 0.35 w/w. The concentration of protein particles in the suspension is 0.0135 w/w, which corresponds to the concentration of protein, 0.01 w/w. For simplicity the intrinsic attenuation in protein particles was neglected.

temperature 25 °C. The calculations were performed with HR-US particle sizing module (2.28.0.1) of a HR-US 102 spectrometer (Sonas Technologies Ltd.), which utilised the equations based on those discussed earlier (Buckin and Altas, 2017; McClements and Coupland, 1996; McClements et al., 1999). An increase or decrease in the frequency results in a shift of the position of the bell-type curves on the particle size scale to the left or to the right. According to Fig. 2, appropriate deconvolution of the thermal and the visco-inertial scattering contributions allow for ultrasonic analysis of particle sizes within 10 nm to 10 μm range (approximately).

The major effects of molecular processes on ultrasonic velocity can be discussed within the framework of the Newton–Laplace relationship for ultrasonic velocity in liquids (Pierce, 1991; Morse and Ingard, 1986):

$$u = \frac{1}{\sqrt{\beta'_S \rho}}, \tag{4}$$

where β'_S is the real part of the adiabatic compressibility of the medium $\beta_S = -\frac{1}{V}(\frac{\partial V}{\partial P})_S = \frac{1}{K_V}$, where P is the pressure applied to the volume of the medium V, and S the entropy of the volume V. This equation is a simplification of Eq. (3) for a limited level of attenuation ($\frac{\alpha\lambda}{2\pi} \ll 1$) in liquids ($G' \ll K'_V$) homogenous within the length scale of the shear wave (the inertial density ρ_I is equal to the gravimetric density of the medium ρ; Buckin, 2012). The compressibility β'_S is adiabatic as at ultrasonic frequencies (up to hundreds of megahertz) the rate of compressions of the medium in the ultrasonic wave is significantly higher than the rate of heat dissipation from the compressed volume (Buckin, 2012). The compressibility β'_S is mainly determined by the intermolecular forces resisting compression of the medium in the ultrasonic wave. The processes outlined above, which contribute to the ultrasonic attenuation, also determine ultrasonic velocity. These contributions, however, are often small. An example of the scattering contribution to ultrasonic velocity in a dispersion of hydrated protein particles calculated with HR-US particle sizing module is presented in Fig. 2.

High sensitivity of compressibility β'_S to molecular organization and intermolecular interactions in the medium allows application of the HR-US technique in analysis of a broad range of molecular processes. This includes analysis of conformational transitions of polymers (Ochenduszko and Buckin, 2010; Perinelli et al., 2017; Van Durme et al., 2005; Wang et al., 2006), ligand binding (Jager et al., 2005; Kargerová and Pekař, 2014; Melikishvili et al., 2016), self-

assembly and aggregation (Andreatta et al., 2005; Dalgleish et al., 2005; Klučáková and Věžníkova, 2016; Lehmann and Buckin, 2005), crystallisation and gelation (Lawrence et al., 2005; Lehmann et al., 2004; Smyth et al., 2001, 2004; Yuno-Ohta et al., 2016; Dalgleish et al., 2004), analysis of phase transitions and phase diagrams (Hickey et al., 2006, 2010), monitoring of chemical and biochemical reactions (Altas et al., 2016; Buckin and Altas, 2017; Resa and Buckin, 2011; Yuelong and Buckin, 2016), and others. Examples of these applications are outlined in Sect. 4.

3 Key attributes of HR-US instruments

HR-US instruments employ novel principles of measurements of ultrasonic parameters based on a combination of interferometric technologies (Buckin and Smyth, 1999) with digital electronic vector analysis. The effective path length travelled by the ultrasonic wave in the sample exceeds the size of the HR-US cell (sample chamber), thus enabling ultrasonic measurements with exceptionally high precision, down to 0.2 mm s^{-1} for ultrasonic velocity, in a broad range of sample volumes, from 0.03 mL (droplet size) to several millilitres with a typical frequency range 1 to 20 MHz (Buckin and Smyth, 1999; Buckin and O'Driscoll, 2002). In addition, the geometry of HR-US ultrasonic cells is optimised for easy filling, refilling, cleaning and sterilisation. They can accommodate aggressive liquids, such as strong acids or volatile organic solvents, without evaporation during a course of measurements. HR-US measurements can be performed over a wide range of temperatures (−40 to 130 °C) at ambient or elevated pressures in static and flow-through regimes, and in different media ranging from dilute solutions to semi-solid materials (Buckin and O'Driscoll, 2002). The measurements can include automated precision titrations of the analysed liquids with a titrant (Jager et al., 2005) and also programmable temperature ramps for temperature profiling. These qualities enable the application of the HR-US technique for non-destructive real-time monitoring of molecular processes in a variety of media and environmental conditions in research, product development, and quality and process control.

4 Examples of applications of HR-US

4.1 Biocatalysis

High-resolution ultrasonic spectroscopy can be successfully employed for real-time, non-destructive analysis of reactions catalysed by enzymes and other catalysts in solutions and complex liquid dispersions. The technique provides precision reaction progress curves (concentration of reactant or product vs. time) over the whole course of reaction, and also can be utilised for analysis of structural rearrangements (e.g. change of particle size) during reactions (Dwyer et al., 2005). In contrast to traditional spectroscopic techniques, HR-US does not require optical transparency or optical markers and is applicable for monitoring of reactions in continuous media and in micro- or nano-bioreactors (e.g. nano-droplets of microemulsions) (Buckin and Atlas, 2017). The accuracy of commercial high-resolution ultrasonic spectrometers in measurements of a change in ultrasonic velocity (down to 0.2 mm s^{-1}; Buckin and O'Driscoll, 2002) corresponds to a μM level of precision in monitoring of the evolution of the concentrations of reactants and products (Resa and Buckin, 2011; Altas et al., 2016; Yuelong and Buckin, 2016). This precision stands for mixtures with low and high concentration of substrates, which allows for monitoring of "low-yielding" reactions (Buckin and Altas, 2017). High precision is important for obtaining of the detailed "reaction rate vs. concentration" profiles over the whole course of reaction utilised in advanced modelling of reaction kinetics and inhibition effects (Resa and Buckin, 2011). Other useful capabilities of the technique include measurements with programmable temperature profiles for assessments of reversible and non-reversible effects of thermal history on enzyme and catalyst activity in a single sample (Altas et al., 2016). Since most chemical reactions in liquids are accompanied by hydration or solvation processes affecting the compressibility, the HR-US technique is applicable for monitoring of a broad range of reactions catalysed by enzymes and other catalysts in various media. Importantly, the ultrasonic analysis can be carried out directly on intact samples with native substrates, thus allowing optimal application of catalysts in targeted media. Two examples of HR-US monitoring of chemical reaction are outlined below.

4.1.1 Hydrolysis of proteins

Hydrolysis of proteins catalysed by proteases is utilised in various industries, from food to effective therapeutics, since the products of this reaction have additional nutritional and functional value. Enzymatic protein hydrolysates containing short-chain peptides with characteristic amino acid composition and defined molecular size are highly desired for specific formulations, since they possess higher solubility, heat stability, and valuable bioactive properties (Chae, 1998; Clemente, 2000). These hydrolysates play important roles in health and well-being, including mineral binding, immunomodulatory, antioxidative, antithrombotic, hypocholesterolemic and antihypertensive functions (Korhonen, 2009). Development and production of protein hydrolysates are dependent on efficient tools for real-time monitoring of the hydrolysis of peptide bonds under different environmental conditions in bioreactors. The results discussed in this chapter illustrate the potential of application of HR-US technology for this task.

Figure 3a shows the real-time ultrasonic velocity profiles in hydrolysis of a globular protein β-lactoglobulin (from bovine milk) at different concentrations (0.547 and 0.273 mmol kg^{-1}) catalysed by enzyme α-chymotrypsin in 0.1 M potassium phosphate buffer at pH 7.8, 25 °C mea-

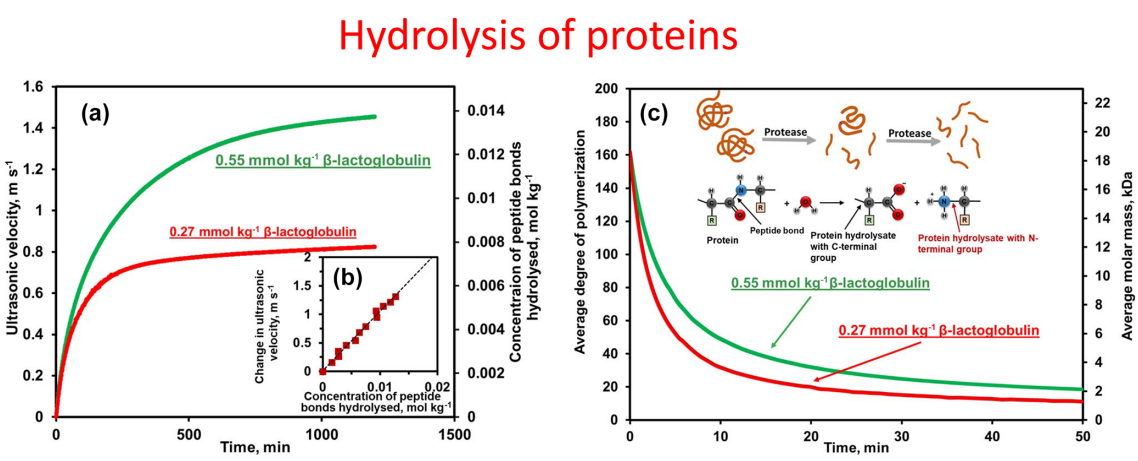

Figure 3. Real-time non-destructive ultrasonic monitoring of hydrolysis of globular protein β-lactoglobulin by enzyme α-chymotrypsin; β-lactoglobulin, 0.55 and 0.27 mmol kg^{-1} in 0.1 M potassium phosphate buffer, pH 7.8, at 25 °C catalysed by α-chymotrypsin from bovine pancreas, 0.01 % w/w. HR-US 102P ultrasonic spectrometer (Sonas Technologies Ltd. Dublin). For more experimental details and data analysis see Buckin and Altas (2017). **(a)** Time profiles of ultrasonic velocity at 15 MHz frequency and of concentration of peptide bonds hydrolysed. **(b)** Calibration of ultrasonic velocity vs. the concentration of peptide bonds hydrolysed as determined by the 2,4,6-Trinitrobenzenesulfonic acid (TNBS) method following the Adler-Nissen protocol (Adler-Nissen, 1979). **(c)** Evolution of average degree of polymerization and molar mass of β-lactoglobulin during hydrolysis calculated from the time profiles of ultrasonic velocity (see Buckin and Altas, 2017, for details).

sured at 15 MHz frequency (Buckin and Altas, 2017). The hydrolysis is described by the following reaction: $P_1{-}C(O){-}NH{-}P_2 + H_2O \rightarrow P_1{-}COO^- + NH_3^+{-}P_2$, where $P_1{-}COO^-$ and $NH_3^+{-}P_2$ represent the protein hydrolysates with C-terminal group and protein hydrolysates with N-terminal group, respectively, and $C(O){-}NH$ represents the peptide bond. The hydrolysis was activated by addition of several microlitres of concentrated solution of an enzyme (α-chymotrypsin from bovine pancreas) to 1.1 mL solution of β-lactoglobulin in 0.1 M phosphate buffer at pH 7.8 preloaded into the ultrasonic cell of a HR-US 102 ultrasonic spectrometer. The concentration of the enzyme in the ultrasonic cell after its addition was 0.01 % w/w.

The hydrolysis is accompanied by a reduction of compressibility of the solution caused by incorporation of one molecule of water into the $-COO^-$ and NH_3^+–atomic groups and by the hydration of these groups (transferring of molecules of bulk water to the hydration shell of these groups). In addition, the intrinsic compressibility of the β-lactoglobulin globule (Kharakoz, 1993, 1997), "removed" from solution during hydrolysis, contributes to the compressibility decrease. The decrease in compressibility of the solution (and accompanied change in density) results in the observed increase in ultrasonic velocity, which can be recalculated into the concentration of peptide bonds hydrolysed (the right y-axis scale of Fig. 3a). The coefficient required for recalculations can be obtained by an appropriate calibration (Buckin and Altas, 2017). Figure 3b shows an example of such calibrations in which ultrasonic measurements were combined with the TNBS (2,4,6-Trinitrobenzenesulfonic acid) discontinuous method (Buckin and Altas, 2017).

The ultrasonically measured concentration of bonds of a polymer or an oligomer, hydrolysed in a course of a reaction, can be recalculated into the change in the average degree of polymerisation and the molar mass during the during the reaction (Buckin and Altas, 2017). Figure 3c illustrates the obtained real-time profiles of those parameters during the first 50 min of the hydrolysis of β-lactoglobulin. The degree of polymerisation at time zero was taken as 162, which corresponds to the number of amino acid residues in β-lactoglobulin. Accordingly, the molar mass at time zero was taken as 18.4 kDa, which represents the molar mass of the 162 amino acids of β-lactoglobulin linked with the peptide bonds between them.

Evolution of ultrasonic attenuation, measured during the process of protein hydrolysis, provides additional information on the mechanism of protein hydrolysis (Buckin and Altas, 2017).

4.1.2 Effects of concentration of enzymes on their activity

The effect of concentration of an enzyme on its activity is an important factor in the developments of enzyme-based formulations. It is commonly assessed by measuring the initial reaction rates in a set of samples containing enzymes of different concentrations. Figure 4 illustrates an alternative methodology for the assessment of the effect of concentration of enzyme lactase (β-galactosidase from *Kluyveromyces lactis*) on its activity in milk. The enzyme hydrolyses β-galactosidic bonds between galactose (Gal) and glucose (R_2) in lactose (a milk sugar). At intermediate stages of hydrolysis, the enzyme produces galacto-oligosaccharides (GOS, β-

linked galactose units, with terminal glucose, including the disaccharide galactose–galactose), which are subsequently hydrolysed (Altas et al., 2016). The hydrolysis of lactose and of the GOS can be described by the following reaction: $Gal{-}O{-}R_2 + H_2O \rightarrow Gal{-}OH + HO{-}R_2$. The reverse reaction represents the synthesis of GOS. This particular enzyme is utilised in formulations for lactose-intolerant infants and is added to milk prior to its consumption for reduction of the level of lactose. The methodology of the analysis of the effect of concentration of β-galactosidase on its activity in milk illustrated in Fig. 4 utilises the titration capabilities of the HR-US technique. The measurements were performed by titration of 1.1 mL of the infant milk in the ultrasonic cell with a concentrated solution of β-galactosidase at 20 °C using pre-programmed precision injections by a HR-US 102 titration accessory. Each injection was followed by a short period of stirring and a period without stirring. The mainframe of the figure shows the ultrasonic velocity profile (secondary y axis) during the time intervals between the stirring periods and subsequent injections. The circles on the inset in Fig. 4 represent the initial rates of hydrolysis obtained from the slopes of linear parts of the dependences at each step of the titration (see Altas et al., 2016, for details) and the triangles show the rates obtained through independent measurements and the reaction profiles in the samples containing enzyme of different concentrations. According to the figure, the reaction rate increases linearly with concentration of the enzyme, thus indicating that the specific activity of the β-galactosidase in the milk does not depend on its concentration within the analysed concentration range.

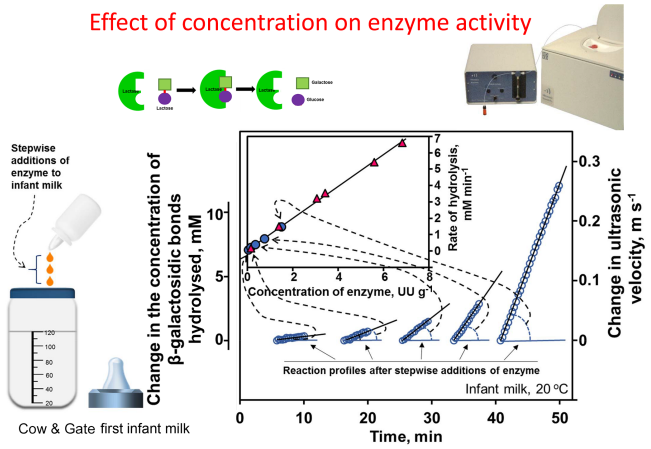

Figure 4. Ultrasonic assessment of effects of enzyme (β-galactosidase) concentration on its activity in hydrolysis of lactose in milk. Main frame: time profiles of ultrasonic velocity and of concentration of β-galactosidic bonds (lactose and GOS) hydrolysed in Cow & Gate First Infant Milk in automatic stepwise injections of β-galactosidase (*Kluyveromyces lactis*) at 20 °C. HR-US 102PT spectrometer equipped with HR-US titration accessory (Sonas Technologies Ltd. Dublin). The ultrasonic measurements were collected in 2 to 15 MHz frequency range. As no significant effects of frequency on the ultrasonic reaction profiles were observed, only the data at 5 MHz are presented. Inset: the initial rates of hydrolysis as function of enzyme concentration; circles – calculated from the data presented in the main frame; triangles – obtained from separate measurements in the samples with different concentration of the enzyme. Adapted with permission from Altas (2016). Copyright ©2016 American Chemical Society.

4.2 Thermal transitions in polymers

Figure 5 illustrates an application of the temperature ramp regime of HR-US spectrometers for analysis of heat transitions in two polymer systems, aqueous solution of poly(N-isopropylacrylamide), PNIPAM, and aqueous solution of egg albumen protein. PNIPAM is a well-known polymer used in thermo-responsive gels and other applications. With temperature, this polymer undergoes a collapse from a random coil into a compact globule accompanied by the formation of aggregates (Van Durme et al., 2005). The transition is marked by a decrease in ultrasonic velocity and an increase in ultrasonic attenuation. The observed decrease in ultrasonic velocity is explained by a dehydration of the atomic groups of the polymer (increase in compressibility of water). The intrinsic compressibility of the globules and aggregates also contributes to the decrease in velocity. The increase in attenuation can be explained by the scattering effects on the aggregates. It is interesting that both parameters change within the same temperature range, thus indicating that the polymer collapse and the aggregation occur simultaneously within the timescale of the measurements. As can be seen from the figure, the ultrasonic profiles provide the transition temperature (half transition point) and the transition temperature interval, which can be utilised in analysis of the energetics of the transition (Gibbs energy, enthalpy) and the cooperativity effects. The measured drop in ultrasonic velocity (when combined with the measurements of density) provides the compressibility of the collapsed or aggregated structure, which can be related to its molecular organisation. The attenuation profile can be recalculated into the size of the aggregates if the required physical properties of the aggregates are known.

In contrast to PNIPAM, the mechanism of the thermal transition (denaturation) in proteins of egg albumen is different. Egg albumen is composed of two major fractions of globular protein, ovalbumin and conalbumin. The first stage of protein denaturation is the unfolding of the globular structure, which is followed by the aggregation of the unfolded proteins caused by the hydrophobic interactions of the exposed hydrophobic side chains of amino acids and other types of interactions. It is interesting to note that despite the different molecular mechanisms of thermal transition, the sign of the change in velocity (decrease) and in attenuation (increase) for egg albumen protein are the same as for PNIPAM. The observed decrease in ultrasonic velocity at transition temperatures can be explained by protein aggregation occurring simultaneously with the unfolding. The

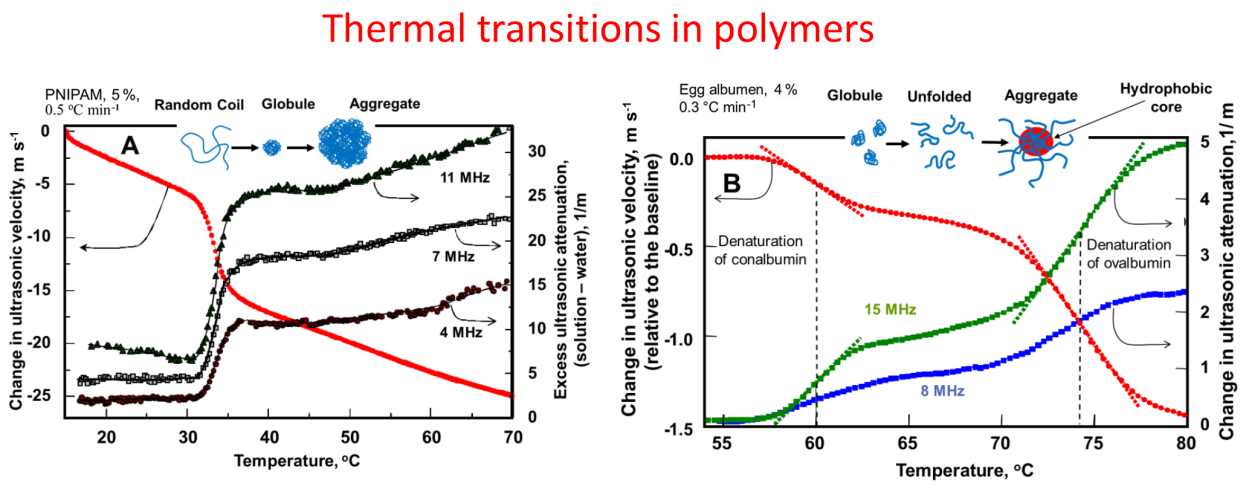

Figure 5. Ultrasonic monitoring of thermal transitions in polymers. **(a)** Thermal transition in aqueous solution of 5 % w/w of poly(N-isopropylacrylamide), PNIPAM. HR-US 102 ultrasonic spectrometer (Ultrasonic Scientific, Dublin), temperature ramp mode, heating rate 0.5 °C min^{-1}. Ultrasonic velocity profile at 7 MHz. No substantial dependence of ultrasonic velocity on frequency within the analysed frequency range, 4 to 7 MHz, was observed. For more experimental details and data analysis see Van Durme et al. (2005). **(b)** Thermal transitions in aqueous solution of 4 % w/w of egg albumin in 0.5 % w/w of NaCl, pH 8.5. HR-US 102P ultrasonic spectrometer (Ultrasonic Scientific, Dublin), temperature ramp mode, heating rate 0.3 °C min^{-1}. Ultrasonic velocity at 15 MHz. No substantial dependence of ultrasonic velocity on frequency within the analysed frequency range, 8 to 15 MHz, was observed. The observed linear decrease in ultrasonic velocity at temperatures before the transition, 50 to 57 °C (not related to denaturation) was extrapolated on the whole temperature range and subtracted as a baseline.

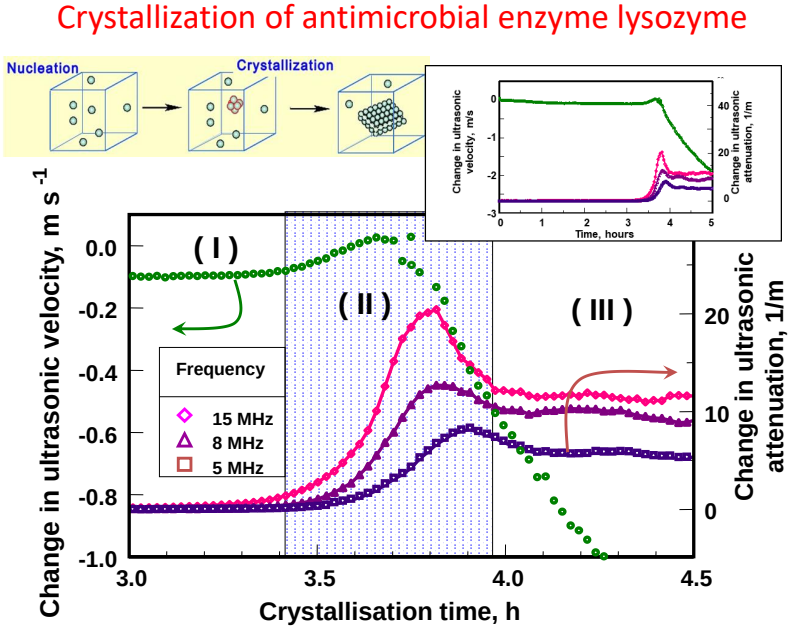

Figure 6. Ultrasonic monitoring of crystallisation of lysozyme. 40 mg mL^{-1} aqueous solution of lysozyme in 0.1 M sodium acetate buffer at pH 4.8 and 20 °C. At time zero a precipitating agent was added to 1 mL of lysozyme solution in ultrasonic cell of a HR-US 102P ultrasonic spectrometer (Ultrasonic Scientific, Dublin) (Lawrence et al., 2005).

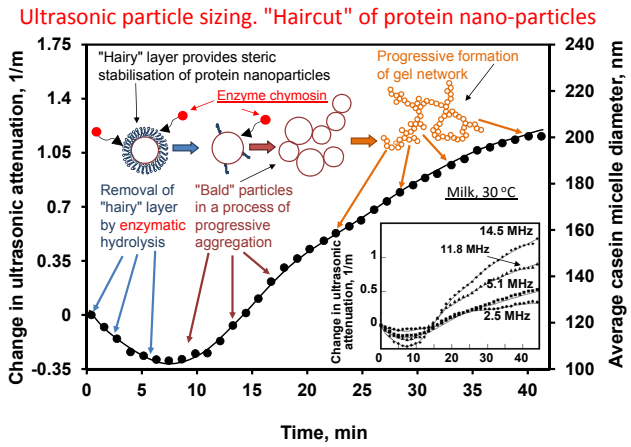

Figure 7. Ultrasonic monitoring of enzymatic haircut of protein nano particles (casein micelles). Main frame: ultrasonic attenuation measured at 14.5 MHz in milk during the renneting process at 30 °C. The enzyme chymosin was added to 1 mL of milk in an ultrasonic cell of a HR-US 102 ultrasonic spectrometer (Ultrasonic Scientific, Dublin). The average particle size was calculated using HR-US particle size software module. Insert: effect of frequency on ultrasonic attenuation profiles measured during renneting of milk at 30 °C. Adapted with permission from Dwyer et al. (2005). Copyright ©Proprietors of Journal of Dairy Research 2005.

aggregation is accompanied by the formation of a "soft", hydrophobic-rich interior of the aggregates, which shall increase the compressibility and decrease the ultrasonic velocity (Ochenduszko and Buckin, 2010). The observed increase in ultrasonic attenuation, as in the case of PNIPAM, can be attributed to the scattering effects on the protein particles. The denaturation profile of egg albumen protein shows two transition temperatures, 60 and 75 °C, which is explained by the presence of two fractions, conalbumin and ovalbumin, with different transition temperatures (Johnson, 1981). When this profile is compared with the profiles of the individual proteins, the effects of the presence of one protein on denaturation parameters and the structure of the aggregates can be evaluated.

4.3 Dynamics of crystallisation processes

Figure 6 shows the real-time ultrasonic monitoring of crystallisation of lysozyme initiated by addition of a precipitating agent to the ultrasonic cell of a HR-US 102P ultrasonic spectrometer containing 1 mL of a 40 mg mL^{-1} solution of lysozyme in a 0.1 M sodium acetate buffer at pH 4.8 at 20 °C (Lawrence et al., 2005). Lysozyme is an antimicrobial enzyme produced by animals that forms part of the innate immune system. By varying the experimental conditions, optimal amounts and sizes of protein crystals can be produced.

The obtained ultrasonic profile shows three stages in the crystallisation process. Over the first 3.4 h of the reaction, a minor decrease in ultrasonic velocity is detected. This could be an indication of processes associated with the effects of the seeding ingredient on the protein molecules. At the end of Stage (I), the ultrasonic velocity and attenuation start to increase, which could be explained by formation of crystals. This increase continues through Stage (II). The rise in ultrasonic attenuation (and the initial rise in velocity) can be attributed to the scattering effects caused by solid crystals formed. During the second half of the Stage (II), the ultrasonic attenuation and velocity start to decrease. At Stage (III), the ultrasonic attenuation nearly levels off, indicating a "saturation" in the process of formation crystals; however, the velocity continues to decrease due to sedimentation of some percentage of crystals from the dispersion.

4.4 Structural rearrangements and particle sizing

Figure 7 illustrates a real-time ultrasonic attenuation profile during enzymatic removal of the "hairy" layer of hydrated protein nanoparticles (casein micelles, approx. 100 nm diameter) at 30 °C (Dwyer et al., 2005). The κ-casein hairy layer on the surface of particles provides the steric stability of the particle dispersion. Its enzymatic removal leads to the particle aggregation and formation of particle gel, which is utilised in cheese making (renneting process).

The measurements were performed in 1 mL of milk (reconstituted from skimmed milk powder) sample using a HR-US 102 ultrasonic spectrometer in a multi-frequency regime in which the data were collected at several pre-selected frequencies between 2 and 15 MHz. The enzyme (rennet, chymosin) was added to milk at time zero. The volume fraction of micelles in the milk, composed of casein and water, was 0.1. The ultrasonic attenuation profiles for different frequencies are presented in the inset, and the profile for frequency 14.5 MHz is plotted in the main frame. This profile was recalculated into the evolution of the "average" (monodisperse) size of the protein particles during the process, using the particle sizing module of HRUS 102 software. The volume fraction of casein micelles was assumed to be constant. The physical parameters of casein micelles and of the continuous medium utilised in these calculations were taken from data published by Griffin and Griffin (1990). Minor amendments of some parameters were introduced to account for small differences in temperature to which the parameters were originally attributed and the temperature at which the measurements were performed (Dwyer et al., 2005).

The particle size scale is presented on the right y axis of the figure. According to the figure the average size of the particles decreases within the first 8 min of the reaction. The decrease in diameter from the initial size (120 nm; Holt, 1986) is approximately 20 nm, which corresponds to the expected thickness of the particle hairy layer (Holt, 1986). This was followed by an increase in the particle size, which demonstrated the beginning of the aggregation of "bald" particles. At the reaction time 30 min, further aggregation of particles results in a formation of a gel network, as indicated by rhe-

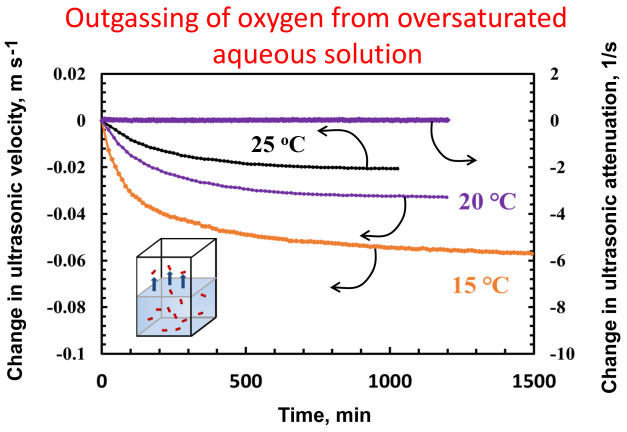

Figure 8. Ultrasonic monitoring of outgassing of oxygen from oversaturated aqueous solution. Evolution of ultrasonic velocity and attenuation (15.1 MHz, 15, 20, 25 °C) of dissolved oxygen during the outgassing process from 1.1 mL of oxygen supersaturated solution in ultrasonic cell of a HR-US 102 ultrasonic spectrometer (Sonas Technologies Ltd. Dublin). The solutions were prepared by fast catalytic decomposition of 20 mM of hydrogen peroxide (Yuelong, 2016).

ological (rise of shear storage modulus) data (Dwyer et al., 2005).

4.5 Monitoring of concentration of oxygen dissolved in water.

The high precision of the HR-US technique in measurements of ultrasonic velocity enables ultrasonic monitoring of concentrations of gases dissolved in liquids. Such measurements are difficult to perform in real time and non-destructively with other analytical techniques, especially if solutions are not at their equilibrium (e.g. oxygenated water oversaturated with oxygen). For example, application of the commonly used electrochemical–electrode technique requires compulsory stirring, which destabilises the solutions and often leads to a dependence of the results of measurements on the speed of flow (Wang and Wolfbeis, 2014; Fondriest Environmental, 2014; Vidal et al., 2003). Also, the electrochemical methods are known to produce incorrect results in the presence of gas bubbles often formed on the surface of electrodes in supersaturated solutions.

Figure 8 illustrates the ultrasonic monitoring of the outgassing of oxygen from super-saturated aqueous solutions in a 1 mL ultrasonic cell at three different temperatures and ambient pressure (Yuelong, 2016). The solutions were prepared by fast decomposition of hydrogen peroxide (20 mM) with enzyme catalase and placed immediately into the measuring ultrasonic cell of a HR-US 102 ultrasonic spectrometer. The measurements of ultrasonic parameters were activated immediately and continued until the ultrasonic velocity reached a plateau, which indicated the full release of super-saturated oxygen. As overall super-saturated solutions of oxygen are unstable, low amplitudes of the oscillations of pressure in the ultrasonic wave were utilised. An absence of the effect of the amplitude (two-fold increase and decrease around the measuring amplitude) on the velocity and attenuation time profiles was confirmed. The ultrasonic velocity profiles can be converted into the concentration profiles of the dissolved oxygen using appropriate calibrations. The measured velocity profiles correspond to the decrease in the concentration of oxygen at levelling-off times by 102, 95 and 78 mg L^{-1} at temperatures 15, 20 and 25 °C. The ultrasonic attenuation was not affected by the outgassing process, which illustrates an absence of formation of gas bubbles in the solution.

5 Conclusions

High-resolution ultrasonic spectroscopy is a capable technique for real-time non-destructive analysis of molecular and micro-structural transformations in research, product development and process control applications. As ultrasonic measurements characterise the properties of the bulk medium, the unwanted effects of surfaces, associated with reflectance spectroscopies and electrode techniques, are excluded. The HR-US technique does not require optical activities, optical markers or other accompanying consumables. This, combined with the ability to perform measurements in opaque samples, in broad temperature ranges, in static and flow-through regimes, in concentrated and in diluted mixtures, and at ambient and elevated pressures, enables application of this technique in a broad range of systems, including those where other analytical methods often fail or have high analytical cost.

Data availability. All relevant data are given in the article or can be found in the cited literature. If required, clarifications of the underlying deltas can be requested by contacting the authors or the manufacturer of HR-US spectrometers, Sonas Technologies Ltd., at www.sonas-group.com.

Competing interests. The author declares that he has no conflict of interest.

Special issue statement. This article is part of the special issue "Sensor/IRS2 2017". It is a result of the AMA Conferences, Nuremberg, Germany, 30 May–1 June 2017.

Acknowledgements. This research has been supported by grant 13F454 from the Department of Agriculture, Food and the Marine of Ireland, H20202 EU Grant 690898 FORMILK. The author is grateful to John Byrne (Crosscare Ltd., Dublin) for his guidance on practical applications of enzyme-based formulations for lactose-intolerant infants, to Sonas Technologies Ltd. for

providing an ultrasonic spectrometer and the accessories for the project, to Evgeny Kudryashov, Shailesh Kumar, Margarida Altas, Yuelong Li, Mark Dizon and Rian Lynch from University College Dublin for their invaluable assistance, and to Ulrich Kulozik from the Technical University of Munich for supplying the samples of egg albumin.

Edited by: Bernd Henning
Reviewed by: two anonymous referees

References

Adler-Nissen, J.: Determination of the degree of hydrolysis of food protein hydrolysates by trinitrobenzenesulfonic acid, J. Agr. Food Chem., 27, 1256–1262, 1979.

Altas, M., Kudryashov, E., and Buckin, V.: Ultrasonic monitoring of enzyme catalysis. Enzyme activity in formulations for lactose intolerant infants, Anal. Chem., 88, 4714–4723, 2016.

Andreatta, G., Bostrom, N., and Mullins, O. C.: High-Q ultrasonic determination of the critical nanoaggregate concentration of asphaltenes and the critical micelle concentration of standard surfactants, Langmuir, 21, 2728–2736, 2005.

Buckin, V.: Application of high-resolution ultrasonic spectroscopy for analysis of complex formulations, Compressibility of solutes and solute particles in liquid mixtures, IOP Conf. Ser.-Mat. Sci., 42, 1–18, 2012.

Buckin, V. and Altas, M.: Ultrasonic monitoring of biocatalysis in solutions and complex dispersions, Catalysts, 7, 1–43, 2017.

Buckin, V. and Hallone, S. K.: Ultrasonic characterisation of W/O microemulsions – structure, phase diagrams, state of water in nano–droplets, encapsulated proteins, Enzymes, in: Microemulsions – An Introduction to Properties and Applications, InTech, 33–66, 2012.

Buckin, V. and O'Driscoll, B.: Ultrasonic waves and material analysis: recent advances and future trends, LabPlus International, 16, 17–21, 2002.

Buckin, V. and Smyth, C.: High-resolution ultrasonic resonator measurements for analysis of liquids, Seminars in Food Analysis, 4, 113–130, 1999.

Chae, H. J., In, M.-J., and Kim, M.-H.: Process development for the enzymatic hydrolysis of food protein: effects of pre-treatment and post-treatments on degree of hydrolysis and other product characteristics, Biotechnology and Bioprocess Engineering, 3, 35–39, 1998.

Clemente, A.: Enzymatic protein hydrolysates in human nutrition, Trends Food Sci. Tech., 11, 254–262, 2000.

Dalgleish, D., Alexander, M., and Corredig, M.: Studies of the acid gelation of milk using ultrasonic spectroscopy and diffusing wave spectroscopy, Food Hydrocolloid., 18, 747–755, 2004.

Dalgleish, D., Verespej, E., Alexander, M., and Corredig, M.: The ultrasonic properties of skim milk related to the release of calcium from casein micelles during acidification, Int. Dairy J., 15, 1105–1112, 2005.

Dwyer, C., Donnelly, L., and Buckin, V.: Ultrasonic analysis of rennet-induced pre-gelation and gelation processes in milk, J. Dairy Res., 72, 303–310, 2005.

Fondriest Environmental: Measuring Dissolved Oxygen, Fundamentals of Environmental Measurements, available at: http://www.fondriest.com/environmental-measurements/equipment/measuring-water-quality/dissolved-oxygen-sensors-and-methods/, last access: 7 January 2014.

Griffin, W. G. and Griffin, M. C. A.: The attenuation of ultrasound in aqueous suspensions of casein micelles from bovine milk, J. Acoust. Soc. Am., 87, 2541–2550, 1990.

Hickey, S., Lawrence, M. J., Hagan, S. A., and Buckin, V.: Analysis of the phase diagram and microstructural transitions in phospholipid microemulsion systems using high-resolution ultrasonic spectroscopy, Langmuir, 22, 5575–5583, 2006.

Hickey, S., Hagan, S. A., Kudryashov, E., and Buckin, V.: Analysis of phase diagram and microstructural transitions in an ethyl oleate/water/Tween 80/Span 20 microemulsion system using high-resolution ultrasonic spectroscopy, Int. J. Pharm., 388, 213–222, 2010.

Holmes, M. and Povey, M.: Ultrasonic Particle Sizing in Emulsions, Ultrasound in Food Processing: Recent Advances, John Wiley & Sons Ltd., Chichester UK, 27–64, 2017.

Holt, C. and Dalgleish, D.: Electrophoretic and hydrodynamic properties of bovine casein micelles interpreted in terms of particles with an outer hairy layer, J. Colloid Interf. Sci., 114, 513–524, 1986.

Jager, M., Kaatze, U., Kudryashov, E., O'Driscoll, B., and Buckin, V.: New capabilities of high-resolution ultrasonic spectroscopy: titration analysis, Spectroscopy, 20, 20–26, 2005.

Johnson, T. M. and Zabik, M. E.: Gelation properties of albumen proteins, singly and in combination, Poultry Sci., 60, 2071–2083, 1981.

Kargerová, A. and Pekař, M.: High-resolution ultrasonic spectroscopy study of interactions between hyaluronan and cationic surfactants, Langmuir, 30, 11866–11872, 2014.

Kharakoz, D. P.: Partial volumes and compressibilities of extended polypeptide chains in aqueous solution: additivity scheme and implication of protein unfolding at normal and high pressure, Biochemistry-US, 36, 10276–10285, 1997.

Kharakoz, D. P. and Sarvazyan, A. P.: Hydrational and intrinsic compressibilities of globular proteins, Biopolymers, 33, 11–26, 1993.

Klučáková, M. and Věžníková, K.: The role of concentration and solvent character in the molecular organization of humic acids, Molecules, 21, 1–10, https://doi.org/10.3390/molecules21111410, 2016.

Korhonen, H.: Milk-derived bioactive peptides: from science to applications, J. Funct. Foods, 1, 177–187, 2009.

Kudryashov, E., Smyth, C., O'Driscoll, B., and Buckin, V.: High-resolution ultrasonic spectroscopy for analysis of chemical reactions in real time, Spectroscopy, 18, 26–32, 2003.

Lawrence, J., Smyth, C., O'Driscoll, B., O'Reagan, T., Hickey, S., and Buckin, V.: High-resolution ultrasonic spectroscopy: analysis of microemulsions, Spectroscopy, 20, 44–49, 2005.

Lehmann, L. and Buckin, V.: Determination of the heat stability profiles of concentrated milk and milk ingredients using high resolution ultrasonic spectroscopy, J. Dairy Sci., 88, 3121–3129, 2005.

Lehmann, L., Kudryashov, E., and Buckin, V.: Ultrasonic monitoring of the gelatinisation of starch, in: Trends in Colloid and Interface Science XVI, edited by: Miguel, M., and Burrows, H. D., Springer, Berlin, Heidelberg, 136–140, 2004.

Litovitz, T. A. and Davis, C. M.: Physical Acoustics, Academic Press, New York, 1964.

McClements, D. and Coupland, J.: Theory of droplet size distribution measurements in emulsions using ultrasonic spectroscopy, Colloid. Surface. A, 117, 161–170, 1996.

McClements, J., Hemar, Y., and Herrmann, N.: Incorporation of thermal overlap effects into multiple scattering theory, J. Acoust. Soc. Am., 105, 915–918, 1999.

Melikishvili, S., Poturnayova, A., Ionov, M., Bryszewska, M., Vary, T, Cirak, J., Muñoz-Fernández, M. Á., Gomez-Ramirez, R., de la Mata, F. J., and Hianik, T.: The effect of polyethylene glycol-modified lipids on the interaction of HIV-1 derived peptide–dendrimer complexes with lipid membranes, BBA-Biomembranes, 1858, 3005–3016, 2016.

Morse, P. M. and Ingard, K. U.: Theoretical Acoustic, Princeton University Press, McGraw-Hill, NY,, 1986.

Ochenduszko, A. and Buckin, V.: Real-time monitoring of heat-induced aggregation of β-lactoglobulin in aqueous solutions using high-resolution ultrasonic spectroscopy, Int. J. Thermophys., 31, 113–130, 2010.

Perinelli, D. R., Cespi, M., Bonacucina, G., Rendina, F., and Palmieri, G. F.: Heating treatments affect the thermal behaviour of doxorubicin loaded in PEGylated liposomes, Int. J. Pharm., 534, 81–88, 2017.

Pierce, A. D.: Acoustics, An Introduction to Its Physical Principles and Applications, Acoustical Society of America, NY, 1991.

Povey, M. J.: Ultrasonic Techniques for Fluids Characterization, Academic Press Limited, London, UK, 1997.

Povey, M. J. and Mason, T. J.: Ultrasound in Food Processing, Springer, Berlin, Germany, 1998.

Resa, P. and Buckin, V.: Ultrasonic analysis of kinetic mechanism of hydrolysis of cellobiose by beta-glucosidase, Anal. Biochem., 415, 1–11, 2011.

Smyth, C., Kudryashov, E. D., and Buckin, V.: High-frequency shear and volume viscoelastic moduli of casein particle gel, Colloid. Surface. A, 183, 517–526, 2001.

Smyth, C., O'Driscoll, B., Lawrence, J., Hickey, S., O'Reagan, T., and Buckin, V.: High-resolution ultrasonic spectroscopy analysis of microemulsions, Pharmacuetical Technology Europe, 16, 31–34, 2004.

Svanberg, S.: Atomic and Molecular Spectroscopy: Basic Aspects and Practical Applications, Springer, Berlin, Heidelberg, 2003.

Van Durme, K., Delellio, L., Kudryashov, E., Buckin, V., Van Mele, B.: Exploration of high-resolution ultrasonic spectroscopy as an analytical tool to study demixing and remixing in poly(N-isopropyl acrylamide)/water solutions, J. Polym. Sci. Pol. Phys., 43, 1283–1295, 2005.

Vidal, J.-C., Garcia-Ruiz, E., and Castillo, J.-R.: Recent advances in electropolymerized conducting polymers in amperometric biosensors, Microchim. Acta, 143, 93–111, 2003.

Wang, Q., Tolkach, A., and Kulozik, U.: Quantitative assessment of thermal denaturation of bovine α-lactalbumin via low-intensity ultrasound, HPLC, and DSC, J. Agr. Food Chem., 54, 6501–6506, 2006.

Wang, X.-D., and Wolfbeis, O. S.: Optical methods for sensing and imaging oxygen: materials, spectroscopies and applications, Chem. Soc. Rev., 43, 3666–3761, 2014.

Yuelong, L.: Application of High-Resolution Ultrasonic Spectroscopy for Real-time Non-destructive Monitoring of Processes of Solubilisation of Gases in Liquids, PhD Thesis Doctor of Philosophy, School of Chemistry, National University of Ireland, University College Dublin, 2016.

Yuelong, L. and Buckin, V.: Ultrasonic real-time monitoring of the process of decomposition of hydrogen peroxide in aqueous solutions, Anal. Methods-UK, 8, 4828–4834, 2016.

Yuno-Ohta, N., Kato, T., Ashizawa, S., Kimura, Y., Maruyama, N., and Nishizu, T.: Role of ovomucoid in the gelation of a β-lactoglobulin-ovomucoid mixture, Colloid Polym. Sci., 294, 1065–1073, 2016.